

LDA and PIV Measurements and Numerical Simulation on In-Cylinder Flow Under Steady State Flow Condition

Tomokazu Nomura^{*1}, Yasushi Takahashi^{*2}, Tsuneaki Ishima^{*1} and Tomio Obokata^{*1}

^{*1} Department of Mechanical System Engineering, Gunma University

1-5-1, Tenjin, Kiryu, 376-8515 JAPAN

^{*2} Honda R&D Co., Ltd. Asaka R&D Center, CIS

3-15-1, Senzui, Asaka, 351-8555 JAPAN

ABSTRACT

In the area of the internal combustion engine designing, it is important to control the airflow in engine cylinder and necessary to understand the airflow and combustion by measurements and numerical simulations in order to reduce the exhaust emissions and improve the efficiency. In this report, characteristics of the flow inside an engine cylinder model have been evaluated by a particle image velocimetry (PIV), a laser Doppler anemometer (LDA) and a numerical simulation with PCC (Partial Cells in Cartesian coordinate) method. The PCC method was developed to reduce the input data preparation works by using Cartesian coordinate and partial cells for any geometry. However, applying the PCC method to analyze the turbulent motions of in-cylinder flow, it is necessary to verify the numerical results using the validated experimental data in the processes of calculation.

Many researches were analyzed the flow in engine cylinder by using the LDA and PIV. The PIV is suitable to understand the spatial distributions of mean velocity and turbulence intensity and can measure the integral length scales from spatial correlation measurements. However, in general, PIV has less time resolution than LDA. This means there are many differences between PIV and LDA data in the quality. Then, it is important to clarify the differences in measurement techniques of PIV and LDA to analyze the turbulence motion experimentally. In this study, characteristics of the flow inside a model engine cylinder have been evaluated by experimental and numerical methods. Verifications of the results obtained by PCC method numerical simulations have been also made by the experimental results. Moreover, the integral length scales of turbulence are evaluated by both PIV and LDA. The integral length scales are directly calculated from spatial correlation coefficients in the PIV measurements. For the LDA measurements, length scale is estimated from the assumption of Taylor's hypothesis (Hinze, 1975; Tennekes et al., 1972). Then, the Taylor's hypothesis is evaluated by comparisons of integral length scale acquired by LDA and PIV.

The model engine head, which has two intake valves and transparent cylinder with bore of 75mm and length of 100mm is used in the steady state flow condition. The tests are conducted by single- or dual- valve open conditions with 8mm valve lift under -1470 Pa suction gauge pressure. The comparisons between the PIV and the LDA experiments show almost the same tendencies for mean velocities in the whole experimental region qualitatively and also quantitatively. However, the PIV results for turbulence intensity have a little smaller strength than that of LDA. The differences in the valve open condition are clearly observed in the integral length and time scales that are estimated from the PIV and LDA data respectively. Moreover, as shown in Fig. 1, the integral length scales estimated by using Taylor's hypothesis are about one fourth of PIV results in the whole measuring regions where the relative turbulence intensities are in high level. It is shown that the PIV results are useful for verification of numerical results, which agree reasonably with those of experiments.

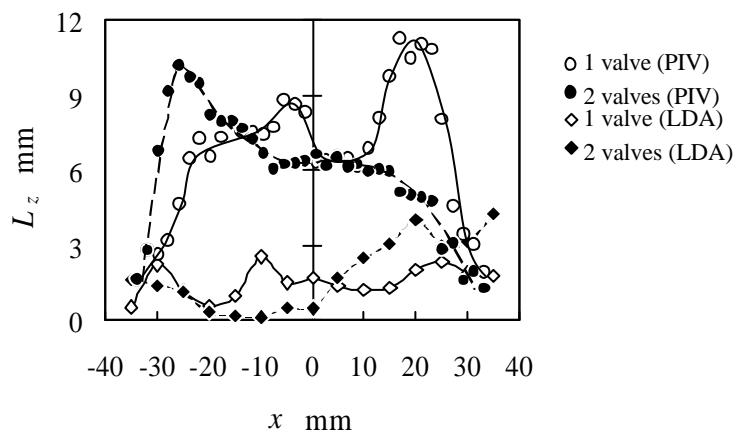


Fig. 1 Comparisons of integral length scale distributions between PIV and LDA measurements at the center plane of $y = 0$ mm.

1. INTRODUCTION

The authors have made experiments about the high pressure fuel spray for direct injection gasoline engine (Ismailov et al., 1999) and a hollow-cone fuel spray for HCCI Diesel engine (Ishima et al., 2003) in order to reduce the exhaust emissions and improve the efficiency of the internal combustion engines. However, to improve the combustion, it is also important to understand and control the airflow in engine cylinder.

In the experimental studies of in-cylinder flow, a laser Doppler anemometer (LDA) and a particle image velocimetry (PIV) are widely used (Josefsson et al., 2001). The LDA and PIV can measure the flow velocity with non-intrusive way and many experimental data have been accumulated in these fields. The LDA has high spatial and temporal resolutions. On the other hand PIV is suitable to understand the spatial distributions of mean velocity and turbulence intensity and can measure the integral length scales from spatial correlations of turbulence. However, in general, PIV has less time resolution than LDA. This means there are many differences between PIV and LDA data in the quality. Then, it is important to clarify the differences in measurement techniques of PIV and LDA to analyze the turbulence motion experimentally.

The characteristics of turbulence time and length scales are very important parameters because the details of turbulence structure can be analyzed by these parameters. Turbulence time scales can be measured by a single point measurement like as hot wire anemometer and LDA since the turbulence time scales can be acquired by using time correlation from time series of velocity fluctuations. On the other hand, turbulence length scales are generally estimated as the product of turbulence time scale and mean velocity by using the Taylor's hypothesis (Hinze, 1975; Tennekes et al., 1972). However, the Taylor's hypothesis cannot be applied in high turbulence flows and it is said the applicable condition is limited in the area where the relative turbulence intensity is less than about 10% and only steady state flow in spatially and temporally. Moreover, two or many points simultaneous acquisitions of velocities are necessary, to measure the integral length scale directly without applying the Taylor's hypothesis. Some LDA systems for measuring spatial correlations are proposed (Fraser et al., 1986; Nakatani et al., 1988) but the studies that measure them directly in real flow fields are very few (Elavarasan et al., 1996). Therefore, it is very important to measure the integral length scale directly and to verify the Taylor's hypothesis in the fluid mechanic researches.

On the other hand, recently, numerical analyses of in-cylinder flow have actively been carried out by a lot of researchers. Direct numerical simulation (DNS) and large eddy simulation (LES) have used in the prediction in-cylinder flow because of great advancements in computer. However, in many cases simply predictions of airflow motion are conducted by using the turbulence model such as $k-\epsilon$. The authors have proposed the PCC (Partial Cells in Cartesian coordinate) method (Takahashi et al., 1994), which only uses Cartesian grids to generate the calculation grid for complicated shapes easily and have applied for the developments of engines head. The numerical simulations using the Cartesian grids have some problems about the calculation accuracy. In particular, in the case to apply the turbulence model, we have some difficulties in the discretization of equations and the calculation methods for the turbulence motions near the wall. Applying the PCC method to numerical simulation, general wall function cannot be used because the cells near the wall have various shapes and sizes. Therefore, a combination of a low Re number $k-\epsilon$ model and the log law equation was proposed for the boundary conditions of turbulence model. The authors already have indicated the validity of this turbulence model and the calculation results in the flow around the rectangular cube mounted on the floor (Nomura et al., 2002). However, applying the PCC method to analyze the turbulent motions in-cylinder flow, it needs the validated experimental data to evaluate the calculation method.

The purposes of this study are to clear the differences in LDA and PIV results at in-cylinder flow under steady state flow condition. Moreover, another one is to verify the numerical accuracies of PCC method applying to complicated geometry flow.

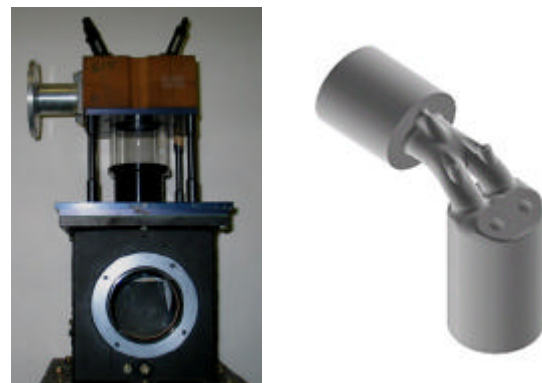
2. EXPERIMENTAL APPARATUS

2.1 Model engine

Figure 2 shows a model engine head used in this study under steady flow condition. This is the four valves SI engine model and two intake ports have the different geometries. It has the transparent cylinder made of the acrylic with bore of 75mm and length of 100mm. This test rig has the outlet box with windows and mirror under the cylinder. The PIV, LDA and flow visualization can be carried out by way of this mirror and windows. The experiments are made by means of sucking the air from the bottom of the cylinder by the blower. The experiments and numerical simulations were conducted by single- or dual- valve open conditions with 8mm valve lift under -1470Pa suction gauge pressure in order to simulate the air flow motion through the intake ports in the actual operating condition. In these conditions, mean velocity at the cross section is about 7.0m/s for dual-valve open condition, and about 4.0m/s for single-valve open condition.

2.2 Particle Image Velocimetry (PIV)

Figure 3 shows the experimental set-up for PIV measurements and table 1 shows the



(a) Test rig.

(b) Solid model.

Fig. 2 Experimental apparatus and solid model of an engine.

specification of PIV. The PIV system consists of an Nd:YAG laser (New Wave Research: Model SOLO III-15), a high-resolution CCD camera (KODAK: MEGAPLUS ES-1.0), a PIV processor (DANTEC: Flow Map 2000) and a personal computer. The laser beams were transformed into light sheets using a cylindrical lens. The high-resolution CCD camera with 1008 x 1018 pixels positioned in a direction normal to the laser sheet. The CCD camera was synchronized with laser pulses and it took two images corresponding to the laser pulses. Each image was divided into the interrogation areas of 32 x 32 pixels with 50% x 50% overlapping. The measuring area is selected as 80mm x 80.8mm and actual interrogation area is 2.5mm x 2.5mm. From each pair of images, two-dimensional vector maps were obtained using a cross correlation method.

2.3 Laser Doppler Anemometer (LDA)

Figure 4 shows the experimental set-up for LDA measurements and table 2 shows the specification of LDA. The LDA system consists of He - Ne gas laser (NEC: GLS3200, 25mW), fiber probe, receiving optics, photomultiplier (DANTEC: 55X08) and counter processor (DISA: 55L90a). The sending optics of LDA had a transmitter lens of 300mm focal length and beam crossing full angle of 7.73 degrees and was applied for double Bragg cell system. The frequency shift was variable and it ranged from 4 to 6 MHz. The measurement was made under the forward scattering one-dimensional mode with 30 degrees of offset angle. The intersection volume size of beams was 95.4 μ m x 1.6mm however real measuring volume size was estimated as 95.4 μ m x 370 μ m under the condition of 30 degrees scattering angle. The seeding particles were water mists whose mean size was about 7 μ m.

Figure 5 shows the measuring points for LDA. The origin was set on the center and the top of the cylinder. The coordinate axes were set to *x*-axis of the radial direction and *z*-axis of the cylinder axis direction. The measurements were made on 6 sections and the measuring points of axial direction were set from *z* = 20mm to *z* = 70mm with 10mm interval. Moreover, the radial measuring points were 5mm interval from a center of the cylinder.

Firstly, as the preliminary experiments, the influences of the sampling frequency of LDA measurements on the mean velocity, turbulence intensity and integral time scale are investigated in order to decide the counter settings. The irregular interval data are acquired by LDA measurements and it is necessary to convert the regular interval data because of applying FFT. Figure 6 shows the influence of the sampling frequency on measurement. These results are measured for flow in *z* direction at *x* = 30mm, *y* = 0mm and *z* = 20mm. In this Figure, the mean velocity and turbulence intensity does not depend on the sampling frequency however the integral time scale shows the large change with changing the sampling frequency. From this result, it

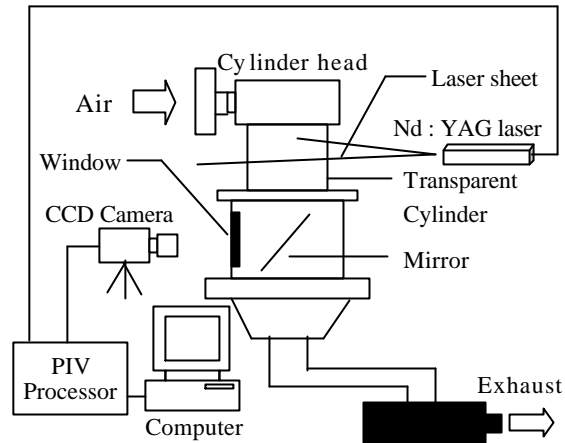


Fig. 3 Experimental set-up for particle image velocimetry.

Table 1 Specification of PIV

Laser source	Nd : YAG
Wavelength (nm)	532
Laser power (mJ)	50
CCD Camera (pixel)	1008 x 1018
Interrogation area (pixel)	32 x 32
Actual Interrogation area (mm)	80 x 80.8
Pulse interval (μ s)	10
Over lap (%)	50 x 50

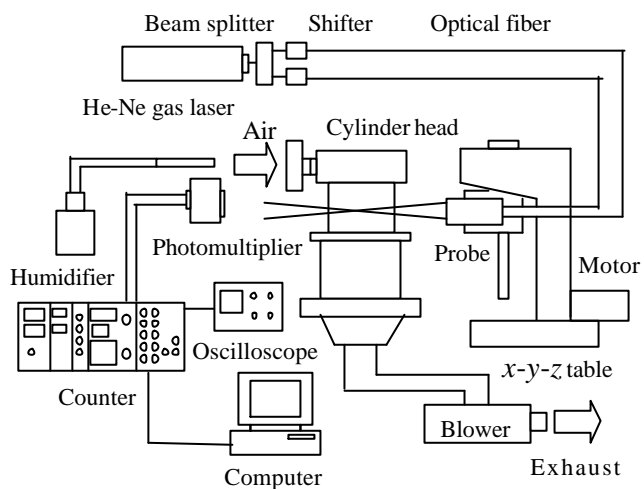


Fig. 4 Experimental set-up for laser Doppler anemometer.

Table 2 Specification of LDA

Laser source	He-Ne
Wavelength (nm)	632.8
Full beam angle (degree)	7.73
Calibration factor (m/s/MHz)	5.21
Mean diameter of waist (μ m)	95.4
Measuring volume length (mm)	1.6
Measuring volume width (μ m)	95.4
Shift frequency (MHz)	4 - 6

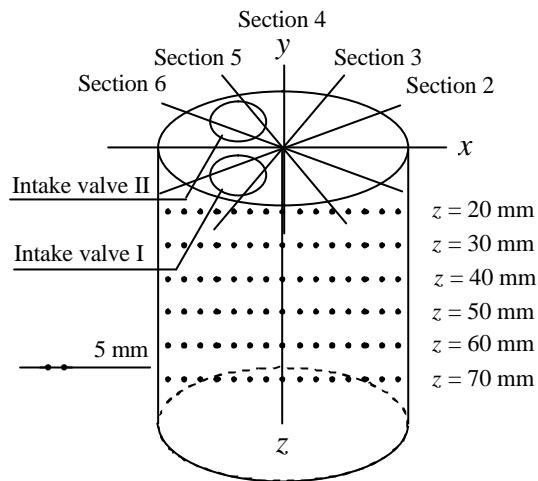


Fig. 5 Measuring points for LDA.

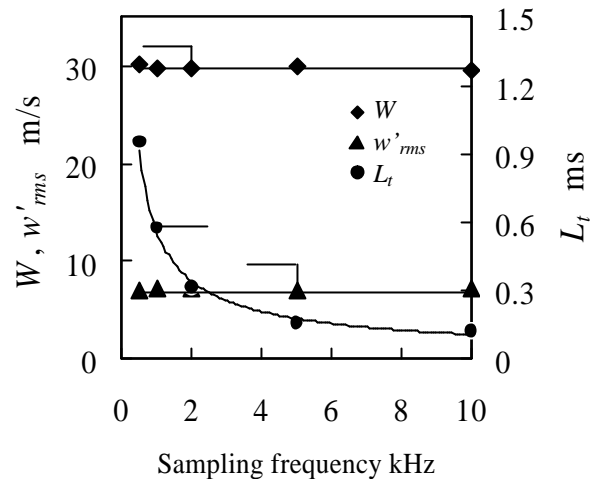


Fig. 6 The influence of the sampling frequency in LDA measurements

seems that it is better to select the larger sampling frequency than 5 kHz that the integral time scale gradient becomes flat. In this study the sampling frequency is set to 10 kHz in measuring the velocity for z direction.

3. NUMERICAL SIMULATION

In this study, numerical simulations of the flow motion in cylinder were conducted on the same condition as the LDA and PIV experiments. The PCC (Partial Cells Cartesian coordinate) method CFD (Computational Fluid Dynamics) code was applied for calculating the flow fields. Only the Cartesian grids were used for a numerical grid generation by the PCC method and it is much easier to generate the numerical grid than that of the BFC (Boundary Fitted Coordinates) method.

When the Cartesian grids are applied for a calculation target, which has the complicated configuration, the cells whose some parts were cut out will be appeared near the wall. These cells are called as "Partial Cell". A general wall function can't be used by the PCC methods because the partial cells have various shapes and a lot of sizes. Therefore a combination of a low Re number $k-\epsilon$ model and log law equation was proposed for the boundary conditions of turbulence model. Moreover, the discretization equations must be derived based on an FVM (Finite Volume Method). SIMPLE (Semi-Implicit Method for Linked Equation) method is utilized as calculation algorithm. A hybrid scheme of first order upwind difference is applied for the convection terms to consider the calculation times and stabilities (Ferziger et al., 1996).

In this study, considering the influence of numerical viscosity, two kinds of numerical grid were used. Figure 7 shows a part of mesh arrangements used in this study. This Figure is the case of the coarse mesh. In another case of fine mesh, the number of cells was about two times as large as that of coarse mesh as to x , y and z direction respectively. The inlet conditions for calculation corresponded to those of the experiments.

4. RESULTS AND DISCUSSIONS

4.1 Vector maps

Figure 8 shows the vector maps at section 1 ($y = 0\text{mm}$) measured by PIV and LDA and calculated by CFD with PCC method. These results are the case of dual intake valves open condition. In the PIV results (Figure 8 (b)), the vortex which located at $x = 0\text{mm}$ and $z = 40\text{mm}$ are recognized. In the LDA results (Figure 8 (a)), the vortex structures are not clear because of coarse measuring intervals, however the flow patterns are similar to the PIV results. The differences between both experimental results are that the PIV results have smaller vectors near the cylinder wall than those of LDA. This is because the PIV could not measure the velocities well near the cylindrical wall as mentioned below. Figures 8 (c) and (d) show the results calculated with coarse mesh and fine mesh respectively. There are slightly differences about the center position of the vortex between both calculations and also from experimental results. The results are caused by that there is not satisfied calculation accuracy due to calculating in whole region which is

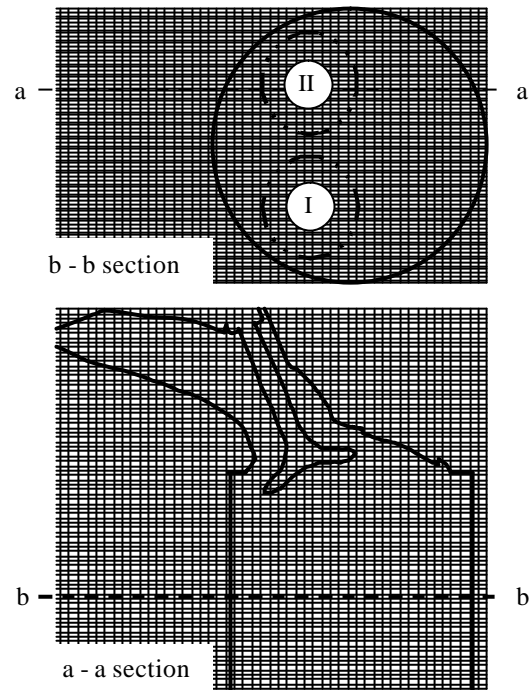


Fig. 7 Mesh arrangement (Coarse mesh).

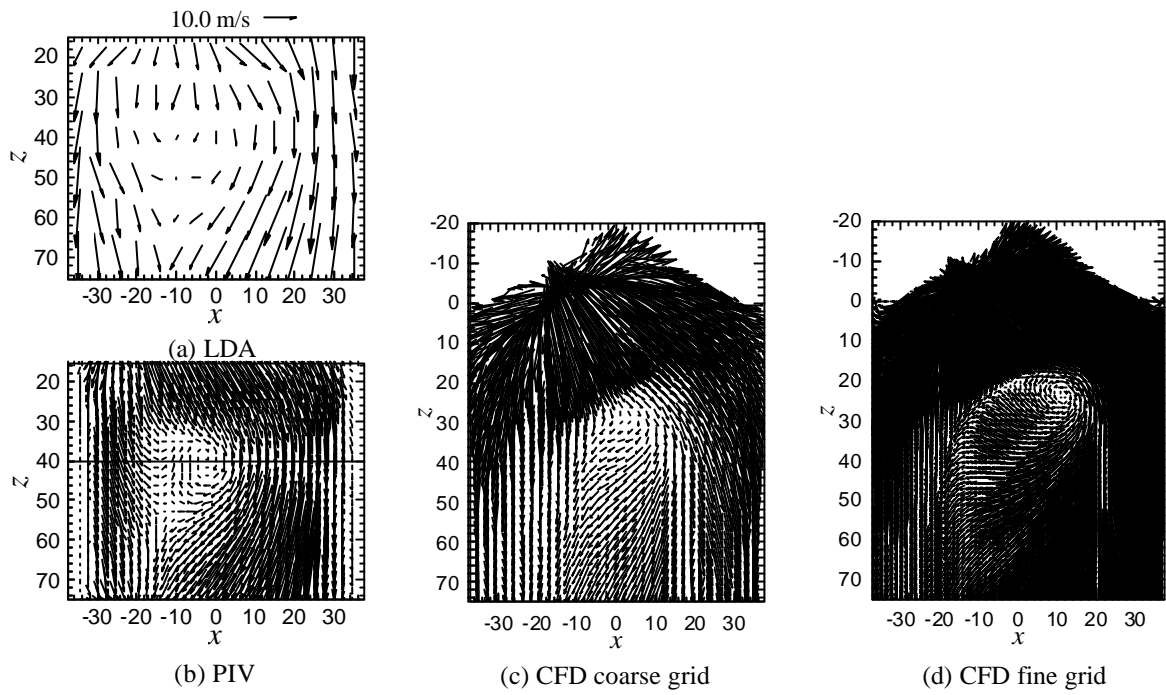


Fig. 8 Comparisons of mean velocity among PIV, LDA and CFD at the center plane of $y = 0$ mm under dual valve open condition.

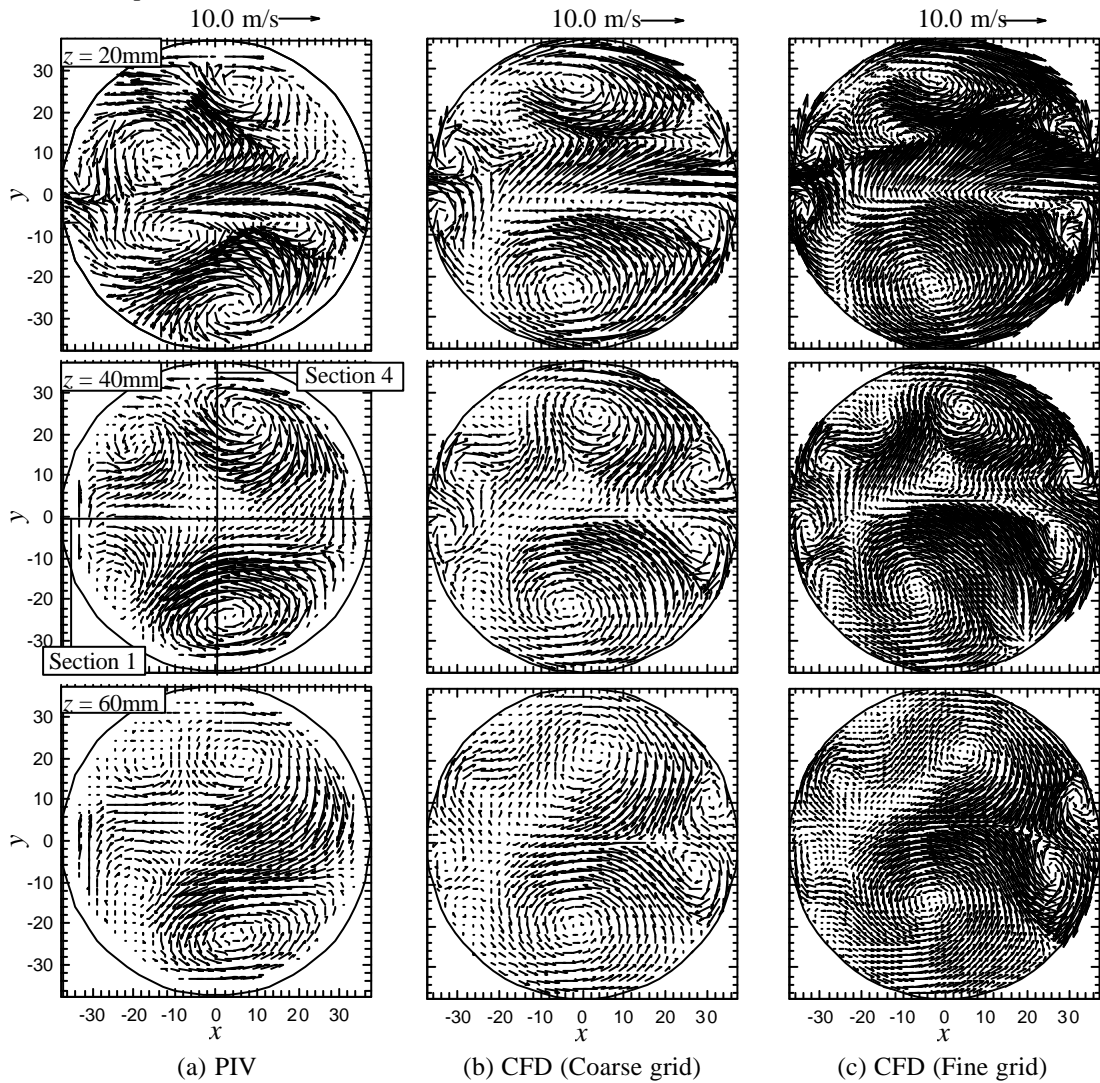


Fig. 9 Comparisons of mean velocities between PIV and CFD at $z = 20, 40$ and 60 mm, top view.

including the intake port and in the surroundings of the intake valves. The vortex center changes by a balance of flows from the two intake ports where CFD can provide less accuracy. The numerical results have larger velocities than those of experiments in the region around $x = -25\text{mm}$ and $z = 25\text{mm}$. It is guessed that these differences are because the separation from an inner wall of intake ports was calculated smaller by CFD. However, both numerical results show as the whole the almost same tendencies as experimental results.

Figure 9 shows the vector maps acquired by PIV and CFD at cross section of cylinder at $z = 20, 40,$ and 60mm . These figures show the results under the dual valves opened condition and are looked from the top of the cylinder. In the PIV results, some vectors near the cylinder wall are rejected because of the deterioration of the image quality by the refraction on cylinder wall and the reflection of laser sheet used for illumination. In both the PIV and numerical results at $z = 20\text{mm}$ cross section, a large scale vortex are recognized around $x = 0\text{mm}, y = -25\text{mm}$ and $x = 0\text{mm}, y = 25\text{mm}$. However, there are small differences about the position at the vortex center between PIV and CFD. The vortex which is recognized at $x = -5\text{mm}$ and $y = -10\text{mm}$ by PIV is not observed clearly by CFD. Only CFD shows the small vortex near the cylinder wall over $x = -30\text{mm}$ and PIV can not catch it clearly because of effects of reflection of laser at cylinder wall and the spatial resolution (the size of interrogation area) in the measurements. Compared with two CFD results which have the different numerical grids, there are a little differences near $x > 0\text{mm}$ and $y = 15\text{mm}$. In the cross section at $z = 40$ and 60mm , it is known that the vortex which is observed at $z = 20\text{mm}$ moved gradually. The PIV and CFD results have a couple of large scale vortex near the $x = 0\text{mm}$ and $y = \pm 25\text{mm}$ and both the size and position of these vortices obtained by CFD are similar to PIV results compared with those at $z = 20\text{mm}$. There are a little

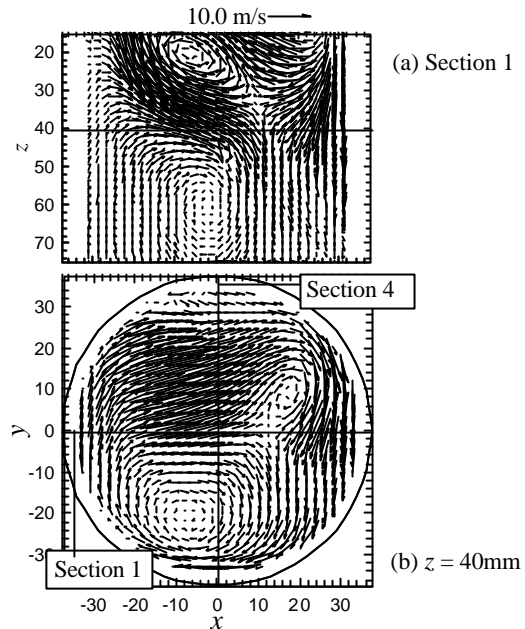


Fig. 10 Mean velocity measured by PIV at the $y = 0\text{mm}$ and $z = 40\text{mm}$ plane under single valve open condition.

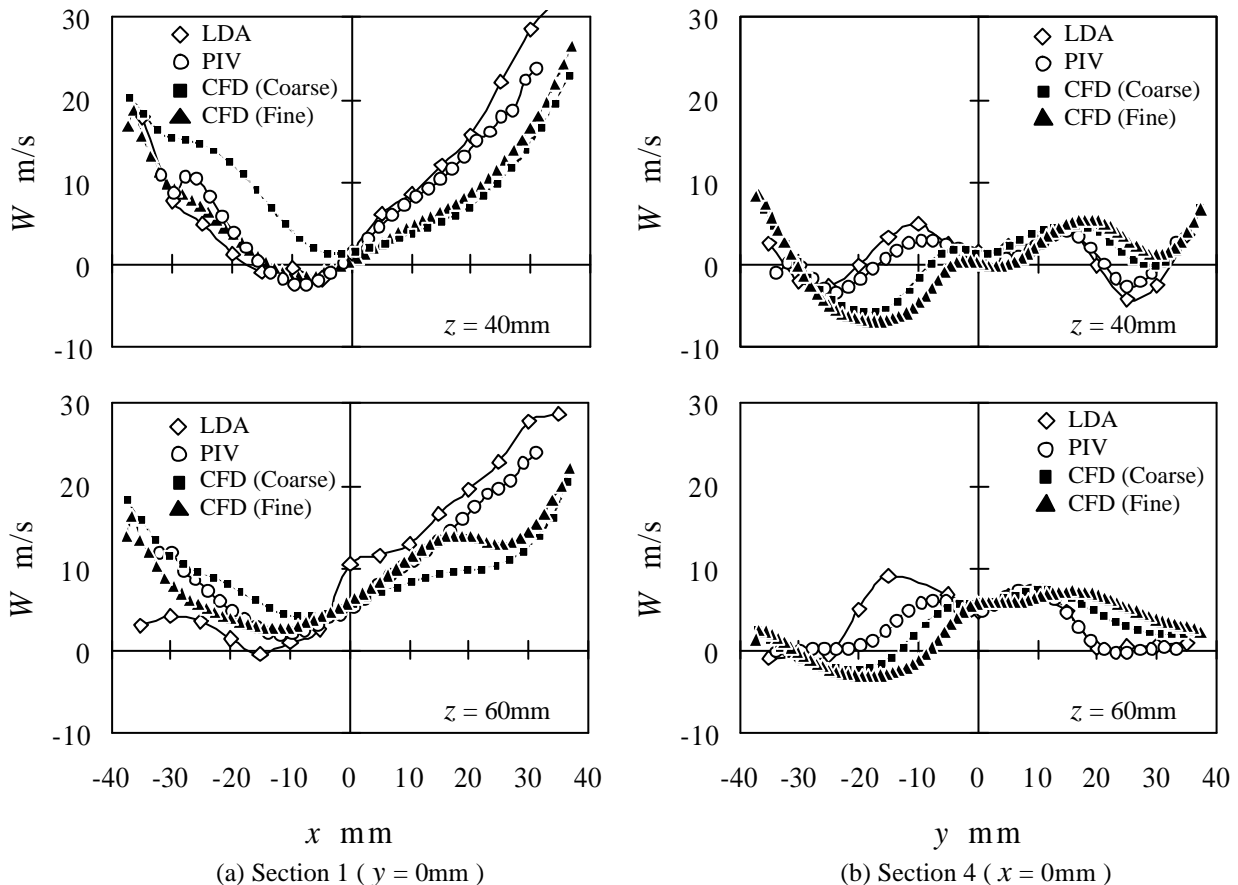


Fig. 11 Comparisons of mean velocity distributions among PIV, LDA and CFD at $y = 0\text{mm}$ or $x = 0\text{mm}$ planes under dual valve open condition.

differences regarding the center positions of vortices between PIV and CFD and these are related to the differences of the vortex position observed at the vertical section as shown in Figure 8. In the flow fields around the obstacle mounted on the floor which are compared with experiments and CFD by the authors (Nomura et al., 2002), the large scale vortex structure observed by calculation with PCC methods was shown larger than those of experiments. The present results have the different tendency compared with them and it is thought that this is a limitation of the calculation of the different flow fields by using the same $k - \epsilon$ turbulent model. Compared with two CFD results, a little difference is observed around $x = 20\text{mm}$ and $y = -30\text{mm}$ at $z = 40\text{mm}$ cross section however the difference can be hardly recognized at both results at $z = 60\text{mm}$ cross section. This is because that three dimensional and small gaps of vortex position in Figure 8 have influenced vector map at cross section. However, both CFD results can reproduce the flow pattern in engine cylinder precisely and it is recognized that the numerical simulation with PCC method is applicable to the analysis for complicated shapes such as intake port, intake valve and cylinder.

Figure 10 shows the vector maps measured by PIV at the single valve (Intake valve II) open state. In the vertical section 1 ($y = 0\text{mm}$) at Figure 10 (a), two vortices, which are centered at $x = -6\text{mm}$, $z = 20\text{mm}$ and $x = -2\text{mm}$, $z = 60\text{mm}$, are observed and flow patterns are more complicated than those of dual valve open state as shown in Figure 8 (b). From the results at $z = 40\text{mm}$ cross section in Figure 10 (b), the larger swirl motion is formed than that of dual valve open state as shown in Figure 8 (b).

4.2 Mean velocity and turbulence intensity distributions

In order to compare with both experiments and CFD in details, the mean velocity (W) distributions and the turbulence intensity (w'_{rms}) distributions for a cylinder axis direction are shown in Figure 11 and 12, respectively. In the section 1 at $z = 40\text{mm}$, the mean velocity acquired by PIV and LDA shows the same distributions and values excepting the near cylinder wall positions. There are some differences between PIV and LDA results only in the region where x is under -10mm at $z = 60\text{mm}$. LDA has the larger velocities than those of PIV near the cylinder wall. This is because in PIV measurements, the good visualization images cannot be acquired by laser reflection from cylinder wall as mentioned before and is also because measurement accuracy deterioration due to a curvature of cylinder. Moreover, two CFD results show the almost same tendencies as both experiments. However CFD results with coarse mesh have gap in position where the velocity becomes in minimum.

In the cross section 4 ($x = 0\text{mm}$) at $z = 40\text{mm}$ as shown in Figure 11 (b) both LDA and PIV results of mean velocity are in good agreement in the distribution. The upward flows to the cylinder axis are observed near $x = \pm 25\text{mm}$

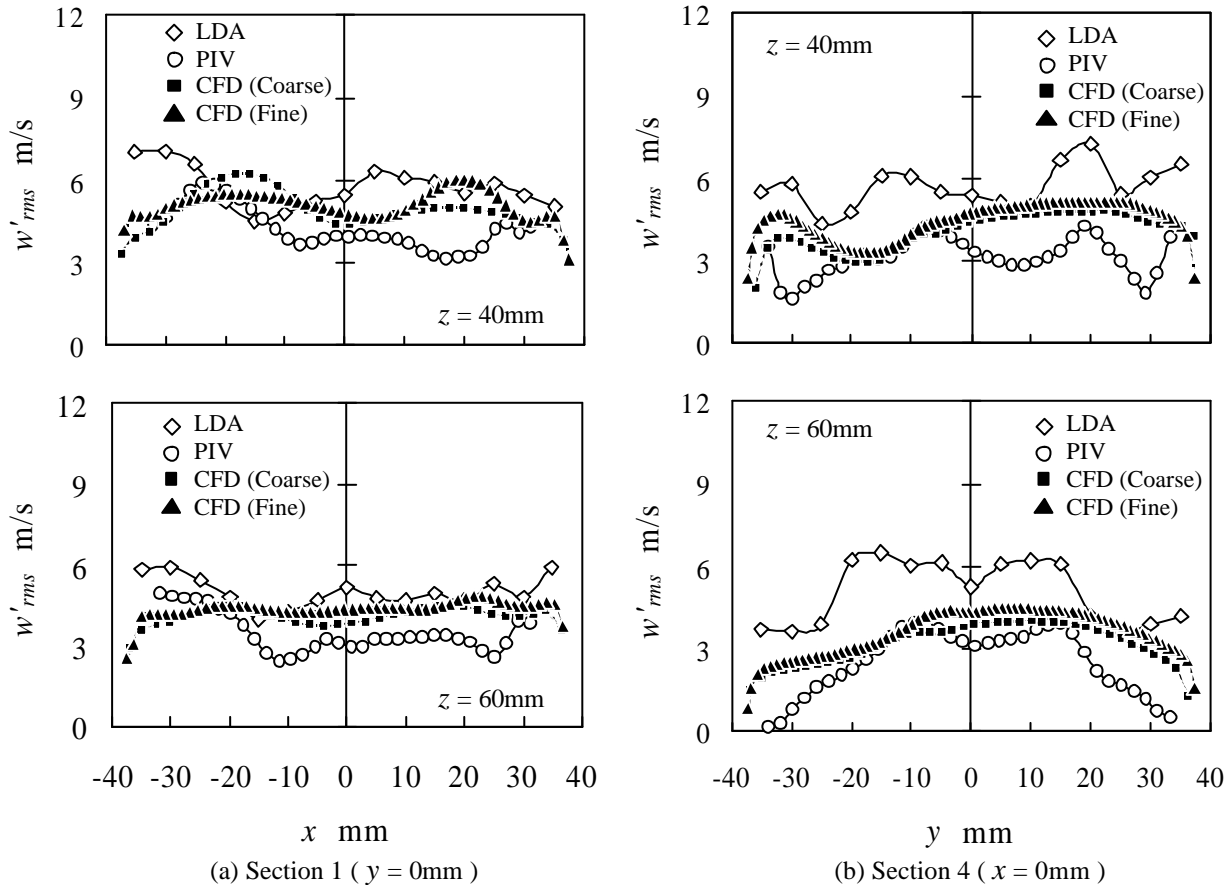


Fig. 12 Comparisons of turbulence intensity distributions among PIV, LDA and CFD at $y = 0\text{mm}$ or $x = 0\text{mm}$ planes under dual valve open condition.

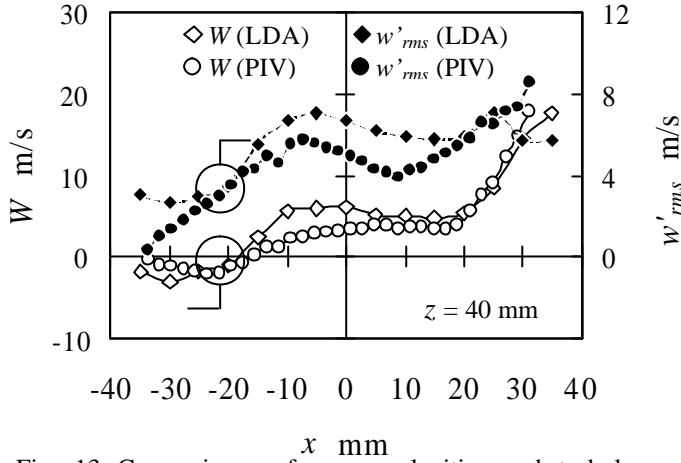


Fig. 13 Comparisons of mean velocities and turbulence intensities among PIV, LDA and CFD at $y = 0\text{mm}$ and $z = 40\text{mm}$ for single valve opening.

and the velocity distribution have the local maximums at $x = \pm 10\text{mm}$ and show the almost symmetric profile with respect to the z axis. There are some differences near $x = -10\text{mm}$ between LDA and PIV results at $z = 60\text{mm}$. CFD results at $z = 40\text{mm}$ and 60mm are different from both experimental results at $y = -20$ to -10 mm however CFD results show the similar velocity distributions to experimental results. The difference in the number of calculation grid does not have the effect on the numerical results.

Regarding as the turbulence intensity, both experimental results have almost similar distributions at section 1 and section 4. However, the PIV results show the 10 to 40% smaller values than those of LDA in whole regions. It is considered that these differences are led to the difference between the measuring volume of LDA and the interrogation area of PIV. In this study, the measuring volume of LDA systems has the width of $95.4\mu\text{m}$ and length of 1.6mm and the actual measuring volume becomes about $95.4\mu\text{m} \times 370\mu\text{m}$ by means of applying the forward scattering system of about 30 degree direction. On the other hand, the interrogation area size of PIV is about $2.6\text{mm} \times 2.6\text{mm}$ and the motions of tracer particles are averaged in the area because of large interrogation area and then the turbulence intensities are shown smaller values than that of LDA. In this case, it is thought that LDA measurements evaluate the turbulence in smaller region than those of PIV.

In the CFD results turbulence intensity for w' component are simply calculated as next equation by means of the assumption of homogenous turbulence.

$$w'_{rms} = (2k/3)^{0.5} \quad (1)$$

Where, k is the turbulence energy. The CFD results show the flat distributions compared with LDA and PIV results however these have the almost same values of both experiments. Moreover, the influences of the difference in numerical grid are small.

Figure 13 shows the only experimental results under single valve open condition at section 1 ($y = 0\text{mm}$) and $z = 40\text{mm}$. These results show the smaller velocities than those of both valve open condition in all regions. This is because the total flow rate has about the half value of both valve open condition due to the constant pressure of the suction and the complicated structures of vortices with larger swirl motion are formed in the single valve open condition.

4.3 Integral scale

Figure 14 shows the spatial correlation coefficients acquired by PIV. These are calculated as based at the cylinder center and $z = 40\text{mm}$ under dual valves open condition. The spatial correlation coefficients $R(r)$ are defined as

$$u_i = U + u'_i \quad (2)$$

$$U = \frac{1}{N} \sum_{i=1}^N u_i \quad (3)$$

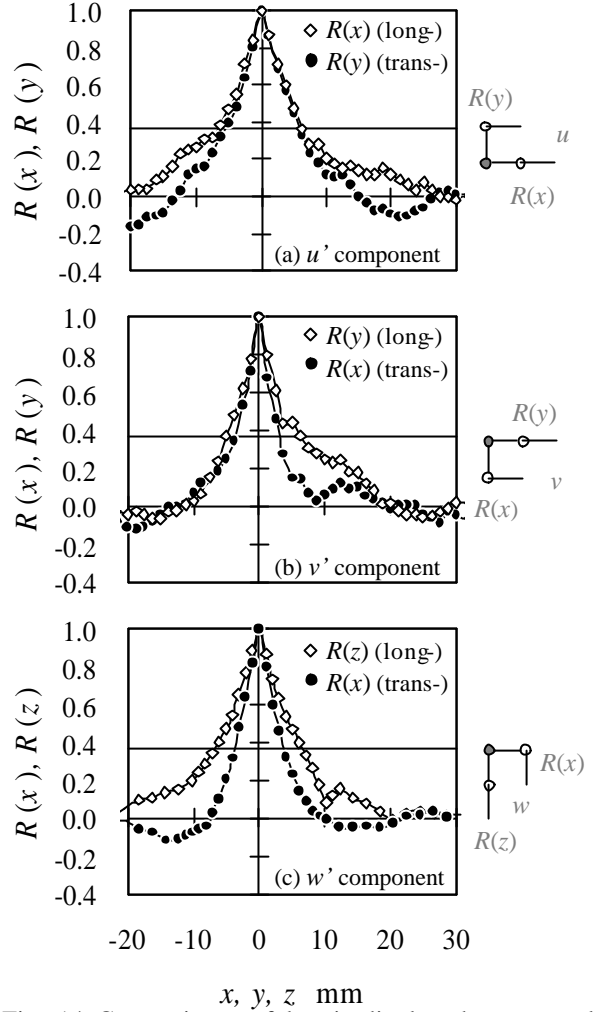


Fig. 14 Comparisons of longitudinal and transversal spatial correlation coefficients measured by PIV under both valve open condition.

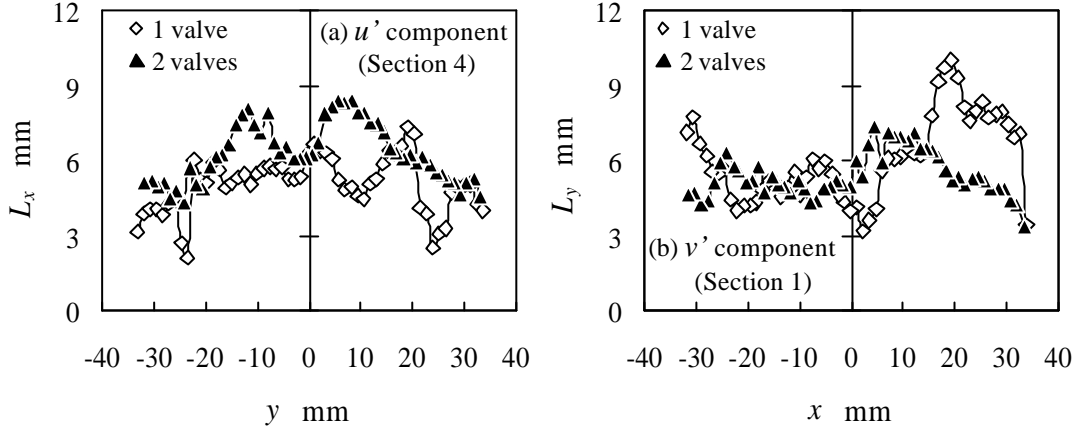


Fig. 15 Longitudinal integral length scale distributions for u' and v' component acquired from the spatial correlation coefficients in Fig. 10.

$$u'_{rms} = \sqrt{\frac{1}{N} \sum_{i=1}^N u_i'^2} \quad (4)$$

$$R(r) = \frac{1}{N} \sum_{i=1}^N \frac{u_i'(\mathbf{x}) \cdot u_i'(\mathbf{x}+r)}{u'_{rms}(\mathbf{x}) \cdot u'_{rms}(\mathbf{x}+r)} \quad (5)$$

Where, N is number of sampling data, u is instantaneous velocity, U is mean velocity and u'_{rms} is turbulence intensity. In all results, spatial correlation coefficient is unity at $r = 0$ and decrease with increasing the distance of measuring points as common tendency. Figure 14(a) shows the spatial correlation coefficients for u' components. The longitudinal correlation coefficients are larger than those of transversal in all measuring area. In the Figure 14(b) for v' components, longitudinal correlation coefficients are larger than those of transversal in the region of positive in x (or y), however both correlation coefficients have the almost same values in the region of negative in x (or y). In the Figure 14(c) for w' components, the results also show the same tendency as u' and v' components and transversal correlation coefficients decayed earlier than those of longitudinal. These results that longitudinal correlations have larger values than transversal ones are same tendencies as common homogeneous turbulence. In these experimental results of spatial correlation for three direction velocity components, transversal correlations are smaller than those of longitudinal and transversal correlation lengths show the half value of longitudinal with the minimum.

Figure 15 shows the integral length scale distributions acquired from spatial correlation coefficients for u' and v' components. These length scales are calculated from the PIV measurements. The integral length scale is defined as

$$L = \int_0^{\infty} R(r) dr \quad (6)$$

In this study, instead of integrating equation (6), the integral length scale L is estimated by correlation length r where $R(r)$ takes the value of $1/e$ ($\cong 0.37$). Figure 15 (a) shows the longitudinal integral length scale (L_x) distributions for u' component at section 4 ($x = 0$ mm) and $z = 40$ mm. These values range from 2 mm to 7 mm in single valve open condition and range from 4 mm to 8 mm in dual valve open condition. The length scale which measured in engine cylinder with motoring condition by G. Valentino ranged from 2 mm to 8 mm (Valentino, et al., 1996) and the results of this study have the almost same value of them. In dual valve open condition L_x has the local maximum values at $y = 10$ mm and -10 mm. These are corresponding to the large velocity regions in Figure 9 (b) measured by PIV. Figure 15 (b) shows the longitudinal integral length scales (L_y) for v' component, L_y has the large value in the region of $x = 20$ mm to 30 mm in the single valve open condition. This is because of the large swirl motion formed in this region. In the other regions, the results of both conditions have almost same values.

Figure 16 shows the integral time scale distributions for w' component measured at section 1 ($y = 0$ mm) and $z = 40$ mm by LDA. The integral time scale is defined as

$$R(\mathbf{t}) = \frac{1}{N} \sum_{i=1}^N \frac{w_i'(\mathbf{x}) \cdot w_i'(\mathbf{x}+\mathbf{t})}{w'_{rms}^2} \quad (7)$$

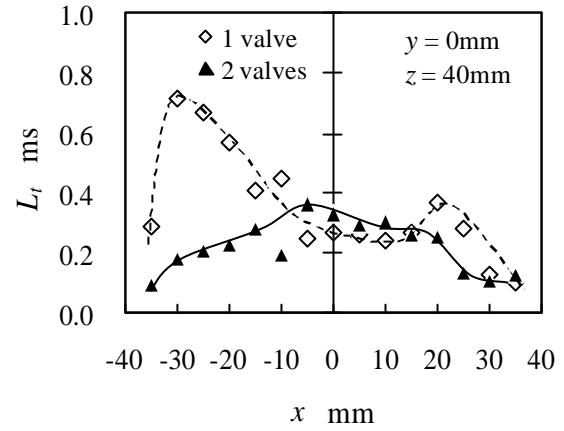


Fig. 16 Variations of integral time scale distributions of w' at the center plane of $y = 0$ mm under single or dual valve open condition.

$$L_t = \int_0^{\infty} R(t) dt \quad (8)$$

Where, $R(t)$ is auto correlation function. Instead of integrating the equation (8), the integral time scale were determined as the time delay t from which $R(t)$ is set to $1/e$ ($\cong 0.37$). In dual valve open condition, the results showed the about 0.1ms to 0.4ms integral time scales and these had the local maximum at the center of the cylinder. On the other hand, in single valve open condition the integral time scale had the larger value than that of another condition near the $x = -30$ mm.

Figure 17 shows the comparisons of longitudinal integral length scale distributions between PIV and LDA. These results are acquired as regards w' component. From the PIV results, the integral scales are calculated by the way of spatial correlation coefficients, as mentioned before. In LDA results, these are estimated by using Taylor's hypothesis as shown next equation.

$$L = L_t \times W \quad (9)$$

Where, L_t is ingeral time scale and W is mean velocity for w' component. The integral length scales have the values less than 4mm in all measuring regions in single and dual valve open states, which are about one fourth values of PIV results. Since the mean velocities show the very small values in the region where x is negative, the length scale estimated by LDA is smaller than that of PIV. It is known that Taylor's hypothesis is applicable to estimate the length scales only in low relative turbulence intensity region under 10%. In this study relative turbulence intensities are over some hundreds % in both conditions and it is considered that the LDA is not able to estimate the integral length scale correctly from the Taylor's hypotesis. It is considered that another reason for the difference is to use the only mean axial velocity (W) as the convection velocity in applying the Taylor's hypothesis in this flow field. However, the real convection velocity will be in more high level because it includes swirl motion.

From the PIV results, in both valve open condition, the length scale distribution has only one peak value in the region where x is negative and it has two peaks in single valve open condition. It is considered that this is reason why the flow patterns are more complicated in single valve open condition than that of both valves open condition as shown in Figures 10(a) and 8(b) respectively.

5. SUMMARY

The in-cylinder flows formed by model cylinder head of engine during the intake process under steady condition were analyzed by PIV and LDA. The verification of CFD results with PCC method was also conducted by the experimental results. These three results were compared in the mean velocity and turbulence intensity distributions. Moreover, the integral length scales were estimated by LDA and PIV and compared each other. The concluding remarks are followings;

1. PIV and LDA results show almost same distributions and values in whole experimental regions regarding to the mean velocity. The PIV results for turbulence intensity have a little smaller value than that of LDA.
2. The transversal correlations of turbulence are smaller than those of longitudinal and transversal correlation lengths show the about half value of longitudinal with the minimum case.
3. The integral length scales of turbulence estimated by LDA results using Taylor's hypothesis are about one fourth of PIV results in the whole measuring regions in the cylinder flow where the relative turbulence intensity is in high levels.
4. Comparing the single valve flow with dual valve open condition, there are many differences not only mean velocity but also turbulence intensity, integral length and time scales.
5. Numerical results by PCC method show little differences in positions of vortices however are in good agreements for the turbulence intensities as well as the flow patterns with experimental results.

Acknowledgement

The authors want to give special thanks to Mr. Chikashi Takeda for his help and advice in this study.

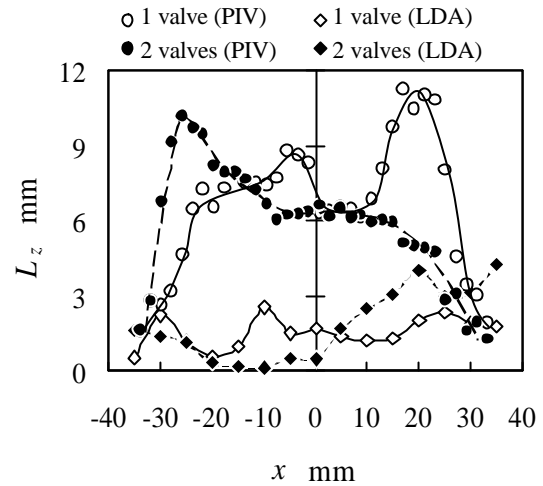


Fig. 17 Comparisons of integral length scale distributions between PIV and LDA measurements at the center plane of $y = 0$ mm.

References

- Elavarasan, R., Djenidi, L. and Antonis, R.A., "A Check of Taylor's Hypothesis Using Two-Point LDV Measurements in a Turbulent Boundary Layer", *Proceedings of 8th International Symposium on Applications of Laser Techniques to Fluid Mechanics*, Lisbon, (1996), pp 29.1.1 -29.1.6.
- Fraser R., Pack, C.J. and Santavicca, D.A., "An LDV System for Turbulence Length Scale Measurements", *Experiments in Fluids*, Vol. 4, (1986), pp. 150-152.
- Ferziger, J.H. and Peric, M., "Computational Methods for Fluid Dynamics Second Edition", (1996), Springer, pp.67-84.
- Hinze, J.O., "Turbulence", (1975), McGraw-Hill Book Company, pp.39-48.
- Ishima, T., Matsuda, T., Shiga, S., Araki, M., Nakamura, H., Obokata, T., Yang, X., Long, W. and Murakami, A., "Characteristics of HCCI Diesel Combustion Operated with a Hollow Cone Spray", JSAE, Paper No. 20030171, SAE Paper No. 2003-01-1823, Yokohama, (2003), pp.1-7.
- Josefsson, G., Fischer, J. and Magnusson, I., "Length Scale Measurements in an Engine Using PIV and Comparison with LDV", *International Symposium on COMODIA*, (2001), pp.653 - 660.
- Ismailov, M.M., Obokata, T., Kobayashi, K. and Polayev, V. M., "LDA/PDA Measurements of Instantaneous characteristics in high pressure fuel injection and swirl spray", *Experiments in Fluids*, Vol. 27, (1999), pp.1-11.
- Nakatani, N., Maegawa, A., Izumi, T. and Yamada, T., "Advancing Multipoint Optical Fiber LDVs - Vorticity Measurement and Some New Optical Systems", *Proceedings of 3rd International Symposium on Applications of Laser Techniques to Fluid Mechanics*, Lisbon, (1988), pp 3-18.
- Nomura, T., Takahashi, Y., Ishima, T. and Obokata T., Analysis on Flow Around a Rectangular Cube by Means of LDA, PIV and the Numerical Simulation by PCC Method –In the Case of Inclined Cube, *Proceedings of 11th International Symposium on Applications of Laser Techniques to Fluid Mechanics*, Paper No. 37.4, Lisbon, (2002), pp.1-11.
- Nomura, T., Takahashi, Y., Ishima, T. and Obokata T., "Analysis on Flow Around a Rectangular Cube by Means of PIV, LDA and Numerical Simulation", *Proceedings of 10th International Symposium on Flow Visualization*, Kyoto, (2002), Paper No. F0136, pp.1-14.
- Takahashi, Y., Fukuzawa, K. and Fujii, I., "Numerical simulation of Flow in Intake Ports and Cylinder of Multi-Valve S. I. Engine using PCC Method", *Proceeding of International Symposium on COMODIA*, (1994), pp.529 - 534.
- Tennekes, H., and Lumley, J.L., "A First Course in Turbulence", (1972), MIT Press, pp.248-256.
- Valentino, G., Auriemma, M., Corcione, F. E., Macchioni, R. and Seccia, G., "Evaluation of Time and Spatial Turbulence Scales in a D. I. Diesel Engine", *Proceedings of 8th International Symposium Applications of Laser Techniques to Fluid Mechanics*, Lisbon, (1996), pp.16.1.1 – 16.1.8.